The Thai Journal of Veterinary Medicine

Volume 52
Issue 3 *52(3)*

Article 8

9-1-2022

Computed tomographic findings of primary renal tumors in dogs and cats

Daji Noh

Jaejin Shim

Sooyoung Choi

Hojung Choi

Youngwon Lee

See next page for additional authors

Recommended Citation

Noh, Daji; Shim, Jaejin; Choi, Sooyoung; Choi, Hojung; Lee, Youngwon; and Lee, Kija (2022) "Computed tomographic findings of primary renal tumors in dogs and cats," *The Thai Journal of Veterinary Medicine*: Vol. 52: Iss. 3, Article 8.
DOI: https://doi.org/10.56808/2985-1130.3242
Available at: https://digital.car.chula.ac.th/tjvm/vol52/iss3/8

Computed tomographic findings of primary renal tumors in dogs and cats

Authors
Daji Noh, Jaejin Shim, Sooyoung Choi, Hojung Choi, Youngwon Lee, and Kija Lee

Original Article

Computed tomographic findings of primary renal tumors in dogs and cats

Daji Noh[1,2] Jaejin Shim[3] Sooyoung Choi[4] Hojung Choi[5] Youngwon Lee[5] Kija Lee[1*]

Abstract

Primary renal tumor is uncommon in dogs and cats, with few previous computed tomography (CT) reports. Previous studies have reported that contrast-enhancing CT is helpful in differentiating the type of renal tumors. This study aimed to describe CT findings of renal tumors in dogs and cats and identify contrast-enhancing pattern according to 3 post-contrast phases. In this retrospective study, the following CT findings were recorded for each patient: (1) renal tumor involvement, (2) enhancement pattern, (3) vascular invasion, (4) presence of lymphadenopathy and organ metastasis, (5) presence of mineralization, and (6) attenuation values of renal tumors on pre- and post-contrast corticomedullary, nephrographic and excretory phase images. Eight dogs and 2 cats met the inclusion criteria, of which 7 had renal cell carcinoma, 2 had lymphoma and one had nephroblastoma. Renal cell carcinomas tended to show heterogeneous and progressive contrast enhancement, unilateral renal involvement and relatively high incidence of lymphadenopathy. Renal lymphomas showed heterogeneous and progressive contrast enhancement and bilateral renal involvement. Nephroblastoma showed heterogeneous and plateau pattern of contrast enhancement and unilateral renal involvement. Findings from the current study support that CT with triphasic contrast study is helpful in renal tumor characterization and vascular invasion and metastasis evaluation. Further large-scale studies are necessary to examine the association between CT and histopathological findings.

Keywords: canine, computed tomography, feline, renal mass

[1]*Department of Veterinary Medical Imaging, College of Veterinary Medicine, Kyungpook National University, Daegu 41566, Korea*
[2]*24 Africa Animal Medical Center, Daejeon 35261, Korea*
[3]*Dodo Animal Clinic, Sacheon 52532, Korea*
[4]*Department of Veterinary Medical Imaging, College of Veterinary Medicine, Kangwon National University, Chuncheon 24341, Korea*
[5]*Department of Veterinary Medical Imaging, College of Veterinary Medicine, Chungnam National University, Daejeon 34134, Korea*
****Correspondence**: leekj@knu.ac.kr* (K. Lee)
Received May 9, 2022
Accepted June 23, 2022
https://doi.org/10.14456/tjvm.2022.57

Introduction

Primary renal tumors are uncommon in small animals, accounting for < 1.7% and 2.5% of all canine and feline tumors, respectively (Bryan JN *et al.*, 2006; Crow SE, 1985). Renal cell carcinoma (RCC) is the most common renal tumor in dogs and lymphoma is the most common in cats (Morris J and Dobson J, 2001). Affected dogs usually have a mean age of 8.4 years, except for those with nephroblastoma with a mean age of 5.2 years (Bryan JN *et al.*, 2006). The mean age of cats with renal lymphoma is 6–7 years but without reported sex predisposition (Mooney SC *et al.*, 1987).

In the veterinary practice, several diagnostic imaging modalities including abdominal radiography, ultrasound and computed tomography (CT) are used for renal masses evaluation (Bryan JN *et al.*, 2006; Haers H *et al.*, 2010; Montinaro V *et al.*, 2013; Tanaka T *et al.*, 2019; Yamazoe K *et al.*, 1994). Radiography and ultrasound are routinely used due to their cost-effectiveness and easy accessibility but are difficult to use in metastasis identification, with nonspecific findings in renal masses differentiation (Haers H *et al.*, 2010). CT examination depicts not only the renal mass but also its adjacent structures more clearly, as well as lungs or lymph node metastasis.

In human, triphasic CT are widely used for renal tumor differentiation due to its provision of characteristic CT findings and contrast enhancement pattern in each tumor, especially in specifying RCC subtype and lymphoma (Kim SH *et al.*, 2016; Muglia VF and Prando A, 2015; Sheth S *et al.*, 2006; Urban BA and Fishman EK, 2020; Wu J *et al.*, 2016; Yuh BI and Cohan RH, 1999). In addition, triphasic CT including corticomedullary, nephrographic and excretory phases are essential for small lesion detection and evaluation of urinary collecting system obstruction (Sheth S *et al.*, 2006). However, in veterinary medicine, only one report has been published on the triphasic CT findings of renal tumors (Tanaka T *et al.*, 2019). The purposes of this study were to describe CT findings of renal tumors in dogs and cats and to analyze contrast-enhancing pattern for each tumor in triphasic contrast study.

Materials and Methods

For this retrospective case series study, the medical databases of the veterinary medical teaching hospitals at the Kyungpook National University between January 2015 and June 2021 were reviewed and dogs and cats with renal tumors were retrieved. Inclusion criteria included (1) presence of renal mass on CT, (2) abdominal contrast-enhancing CT study including arterial, portal-venous and delayed phases, and (3) renal tumor confirmed by cytology and/or histopathology. Medical records with the following data were recorded: signalment, clinical findings on physical examinations, hematological examinations, cytohistological results, survival time and outcome.

Computed tomography scan techniques and image assessment: All dogs and cats were premedicated appropriately, if necessary. Butorphanol (0.2 mg/kg) and midazolam (0.2 mg/kg) in dogs and butorphanol (0.2–0.3 mg/kg) in cats were intravenously injected as premedication. Anesthesia was induced with an intravenous dose of 2 mg/kg of propofol (Provive; Myungmoon Pharm, Seoul, Korea) in dogs and 5 mg/kg of propofol in cats and maintained with 2% isoflurane (Forane; Choongwae Pharm, Seoul, Korea) for the CT scan. The anesthetized dogs and cats were positioned in dorsal recumbency on the CT table. All patients had thoracic and abdominal CT images obtained using a 32-multislice CT scanner (Alexion; Canon Medical System, Otawara, Japan). Scanning parameters were 120 kV, 150-200 mA, 1.0 mm slice thickness, 0.75 s rotation time and craniocaudal scan direction. A contrast study was performed after administration of 600 mgI/kg of iohexol (Bonorex 300 Inj.; Daihan Pharm, Seoul, Korea) via the cephalic vein for 20 s, using an autoinjector (Medrad; Bayer Health Care LLC, Whippany, NJ, USA). Three abdominal CT scans were obtained at 20, 40 and 60 s, respectively, after contrast material injection. Thoracic CT scans for metastasis evaluation were performed at the pre- and post-contrast delayed phase. All CT data was reconstructed to three cross-sectional images (transverse, sagittal, and dorsal planes) using the inbuilt software of the CT scanner.

All images were reviewed using a picture-archiving and communication system (INFINITT Healthcare; Seoul, Korea). All abdominal pre- and post-contrast CT images were evaluated on a soft-tissue window (window width (WW), 450 HU; window level (WL), 40 HU). Thoracic CT images were evaluated on a lung window (WW, 1600 HU; WL, -550 HU), soft-tissue window reconstruction was performed with metastasis suspicion.

CT findings were recorded including renal tumor involvement, enhancement pattern, vascular invasion, lymphadenopathy, organ metastasis and mineralization. Renal tumor involvement was defined as unilateral or bilateral. Enhancement patterns of renal mass were subjectively classified as homogeneous (uniform appearance) or heterogeneous (varied attenuation). The presence of vascular invasion was recorded as presence or absence in the caudal vena cava or renal vein. Presence of adjacent regional lymph node enlargement, organ metastatic lesion and intratumoral mineralization were recorded.

The CT attenuation values of renal masses in the pre-contrast and triphasic post-contrast scans were measured by one author (D.N.) with 7 years of experience in veterinary diagnostic imaging using a circular region of interest (ROI). This ROI was created thrice in each renal mass and the attenuation value was defined as the mean of the three ROI values. In each phase, the circular ROI at the same location was drawn as the largest possible area on the renal mass that included solid tumoral parenchymal but excluded mineral attenuation, blood vessel, cystic lesion and tumor margins. According to CT attenuation values, the time-course contrast enhancement pattern was evaluated from corticomedullary to excretory phases and classified as plateau and progressive. Plateau pattern was defined as attenuation values of renal masses gradually increased to the nephrographic phase and decreased in the excretory phase. Progressive pattern was defined as attenuation values of renal masses gradually increased in all three phases. Other recorded CT findings include the laterality of

renal mass and presence of intratumoral mineralization, adjacent regional lymph node enlargement and pulmonary metastasis.

Results

Eight dogs and 2 cats met the inclusion criteria. Canine breeds included 4 Maltese and one each of Shih-tzu, Schnauzer, Cocker spaniel and Jindo. The two cats included domestic short hair and Persian. Out of 8 dogs, 2 were intact males, 4 neutered males and 2 intact females. The mean age and body weight of 8 dogs was 9.8 ± 3.8 years (range, 2–12.8 years) and 8.6 ± 9.4 kg (range, 2.2–30 kg), respectively. In the 2 cats, one was a neutered female and the other was a neutered male with ages of 2.2 and 12 years old and weights of 3.1 kg and 3.6 kg, respectively. Clinical signs, including anorexia (7/10), weight loss (6/10), vomiting (4/10), palpable abdominal mass (3/10), abdominal pain (1/10), hematuria (1/10), dysuria (1/10), and asymptomatic (1/10) were reported in 8 dogs and 2 cats.

Abnormalities in hematological examinations were nonspecific. One case (Dog 4) had increased lymphocyte counts, 67.7 × 10^9 cells/L (reference range: 6.0–17.0 × 10^9 cells/L). Another (Dog 7) had moderate anemia with 22% of hematocrit (reference range: 37%–55%). Serum chemistry results were normal in 7/9 recorded results. A high serum concentration was observed in dogs and cats including alkaline phosphatase (2/9), blood urea nitrogen (2/9), alanine aminotransferase (1/9), creatinine (1/9), phosphorus (1/9), amylase (1/9) and cholesterol (1/9).

Eight masses in 8 dogs were sampled via gun biopsies (3/8) or fine needle aspiration (5/8). Three of these were submitted for histopathology after nephrectomy and revealed as RCC. Renal nephroblastoma in a dog was diagnosed histopathologically via gun biopsy. All renal lymphoma diagnoses were based on ultrasound-guided fine needle aspiration.

CT findings of renal tumor in the 8 dogs and 2 cats are summarized in Table 1. In addition, attenuation values of the mass on pre- and post-contrast CT are summarized in Table 2. In 7 cases of RCC, 6 dogs revealed heterogeneous mass but one dog revealed homogeneous mass. All these cases had unilateral renal mass; two cases had right masses and five had left masses. Four cases of RCC tended to have progressive contrast enhancement (Fig. 1) and another 3 cases had plateau pattern of contrast enhancement. Mean attenuation values of masses were 35.0 ± 4.0, 86.0 ± 29.2, 119.6 ± 36.5, and 126.4 ± 45.5 HU on pre-contrast, post-contrast corticomedullary, nephrographic and excretory phases, respectively (Table 2).

Table 1 CT features of each renal tumor group

	Number and frequency of renal tumors		
CT features	**Renal cell carcinoma (*n* = 7)**	**Lymphoma (*n* = 2)**	**Nephroblastoma (*n* = 1)**
Renal tumor involvement	Right (2), Left (5)	Bilateral (2)	Left (1)
Enhancement pattern	Homogeneous (1) Heterogeneous (6)	Heterogeneous (2)	Heterogeneous (1)
Vascular invasion[a]	1/7 (14.3%)	0	1
Lymphadenopathy	4/7 (57.1%)	0	1
Organ metastasis[b]	3/7 (42.9%)	0	1
Mineralization	3/7 (42.9%)	0	0

[a] All dogs had caudal vena cava invasion.
[b]All dogs with organ metastasis had pulmonary metastasis

Table 2 Attenuation value of the mass on pre- and post-contrast CT in patients with renal tumor

Case	Diagnosis	CE pattern	Attenuation value (HU)			
			Pre-contrast	Corticomedullary phase	Nephrographic phase	Excretory phase
Dog 1	NB	plateau	35	90	125	110
Dog 2	RCC	progressive	40	45	95	114
Dog 3	RCC	progressive	32	48	64	70
Dog 4	RCC	progressive	37	100	120	146
Dog 5	RCC	progressive	28	120	160	205
Dog 6	RCC	plateau	38	82	108	100
Dog 7	RCC	plateau	35	107	170	155
Dog 8	RCC	plateau	35	100	120	100
Cat 1	Lymphoma	progressive	35	70	90	102
Cat 2	Lymphoma	progressive	34	60	98	106

CE, contrast enhancement; NB, nephroblastoma; RCC, renal cell carcinoma

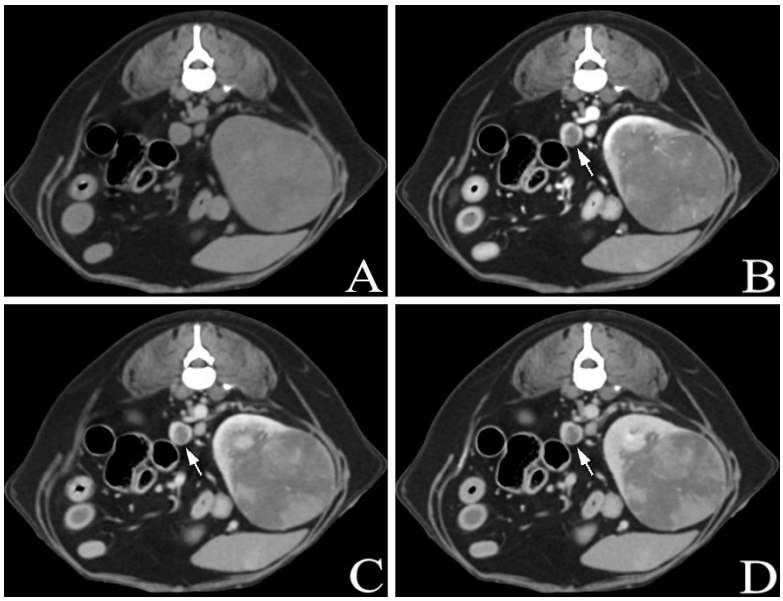

Figure 1 Pre- (A) and post-contrast (B–D) transverse CT of renal cell carcinoma in the left kidney of Dog 2. The mass is heterogeneous, showing a progressive contrast enhancement. Attenuation values on pre-contrast (A), corticomedullary (B), nephrographic (C) and excretory phases (D) are 40, 45, 95, and 114 HU, respectively. Vascular invasion to caudal vena cava is shown (arrows).

CT images of nephroblastoma (Dog 1) showed a large (59 × 95 × 34 mm), irregular, hypoattenuating and heterogeneous mass. This tumor tended to have a plateau pattern on post-contrast scans (Fig. 2). The attenuation value of the mass was 35, 90, 125 and 110 HU on pre-contrast, post-contrast corticomedullary, nephrographic and excretory phases, respectively (Table 2).

CT images of lymphoma in the 2 cats showed hypoattenuating, bilateral and irregular mass with heterogeneous contrast enhancement. A thin peripheral rim of low attenuation corresponding to the necrotic cortex existed with normal enhancing medulla on post-contrast CT. Post-contrast CT scans showed bilaterally enlarged kidneys with lobulated contours and multiple hypoattenuating nodules of varying sizes in the periphery of the kidneys. Both cases of lymphoma tended to have progressive contrast enhancement. The mean attenuation values of masses were 34.5 ± 0.7, 65.0 ± 7.1, 94.0 ± 5.7 and 104.0 ± 2.8 HU on pre-contrast, post-contrast corticomedullary, nephrographic, and excretory phases, respectively (Table 2). Fig. 3 shows the representative images of lymphoma.

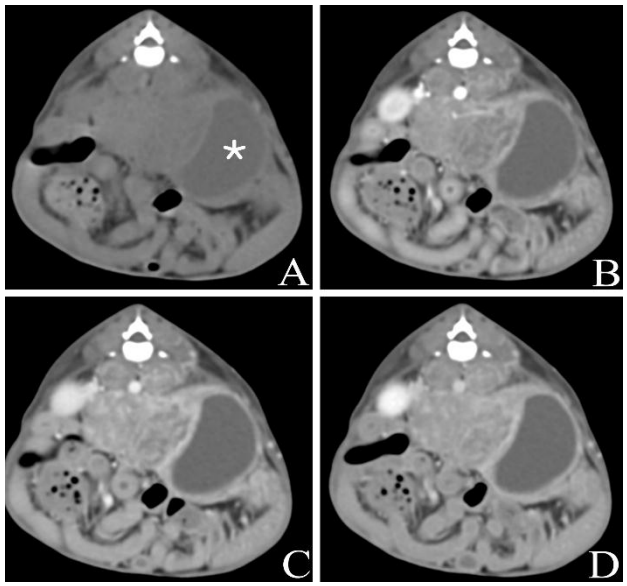

Figure 2 Pre- (A) and post-contrast (B–D) transverse CT of nephroblastoma in the left kidney of Dog 1. CT revealed a large sized, irregular, heterogeneously hypoattenuating mass. A dilated renal pelvis appears as a cyst (asterisk). The mass is heterogeneous and shows plateau pattern of contrast enhancement. Attenuation values on pre-contrast (A), corticomedullary (B), nephrographic (C), and excretory phases (D) are 35, 90, 125, and 100 HU, respectively.

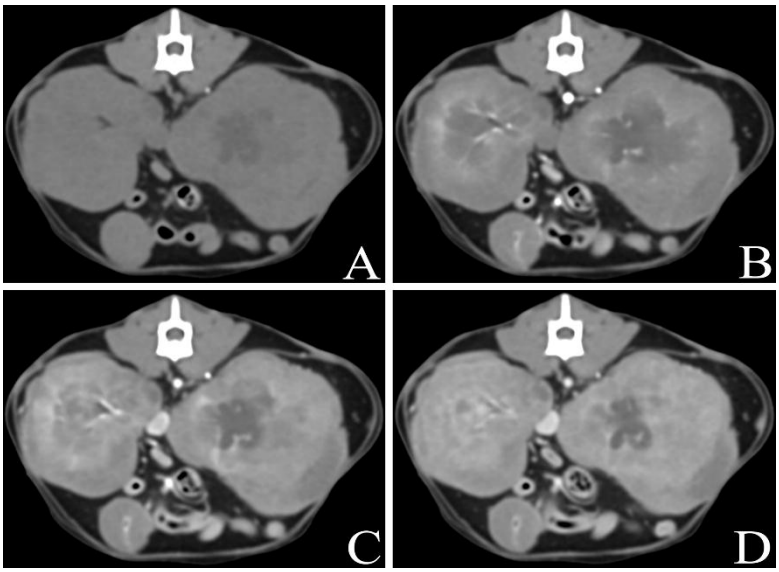

Figure 3 Pre- (A) and post-contrast (B–D) transverse CT of renal lymphoma in Cat 1. The mass is hypoattenuating, bilateral, and irregular with heterogeneous and progressive contrast enhancement. Attenuation values on pre-contrast (A), corticomedullary (B), nephrographic (C) and excretory phases (D) are 35, 70, 90, and 102 HU, respectively.

Invasion of the caudal vena cava was present in one case of RCC and one case of nephroblastoma. Lymphadenopathy was present in 4 cases of RCC and a case of nephroblastoma. Lung metastasis was present in 3 cases of RCC and a case of nephroblastoma, without cases of lymphoma. Mineralization was present in 3 cases of RCC but not in nephroblastoma and lymphoma.

Mean survival time for 7 cases was 46 days (range, 7–90 days). One dog (Dog 8) recovered well from surgery and the dog was in good condition without complications and recurrence or metastasis at 3 weeks follow-up. Follow-up for 2 cases (Dog 7 and Cat 2) were unavailable due to the retrospective features of this study.

Discussion

This study revealed the triphasic CT findings of primary renal tumor and its contrast enhancement pattern in dogs and cats including RCC, lymphoma and nephroblastoma. In veterinary medicine, diagnostic imaging modalities to compare renal tumors and assess the degree of vascularization are contrast-enhanced ultrasound (Haers H *et al*., 2010) and triphasic contrast-enhanced CT (Tanaka T *et al*., 2019). In a previous study using contrast-enhanced ultrasound, the RCC had characteristic contrast features that differed from other renal tumors including histiocytic sarcoma, lymphoma and metastatic nodules (Haers H *et al*., 2010). However, contrast-enhanced ultrasound is not enough for tumor differentiation with overlapped findings with different histotypes, even in human clinical practice (Bertolotto M *et al*., 2018). Meanwhile, triphasic contrast-enhanced CT in human medicine are used to differentiate renal tumor by typical contrast enhancement pattern while definitive diagnosis is made by cytohistological examination (Kim SH *et al*., 2016; Muglia VF and Prando A, 2015; Sheth S *et al*., 2006; Urban BA and Fishman EK, 2020; Wu J *et al*., 2016; Yuh BI and Cohan RH, 1999). In dogs, only one study has been reported comparing the triphasic contrast-enhanced CT findings of primary renal tumor that revealed variable tumoral and vessel enhancement in RCC, lymphoma and hemangiosarcoma (Tanaka T *et al*., 2019). However, triphasic contrast-enhanced CT findings of primary renal tumor in dogs and cats are still lacking, thus this retrospective study was performed.

The attenuation values on post-contrast CT studies are related to the amount of iodine deposited in a target organ or the intravascular blood volume affected by numerous factors including patient-related and injection-related factors. Patient-related factors include the body size (height and weight) and cardiac output. Body weight is an important factor affecting the attenuation values on the post-contrast CT image. Large subjects have larger blood volumes as compared to small subjects, causing dilution of contrast medium that leads to lower contrast enhancement (Bae KT, 2010; Herman S, 2004). Injection-related factors include volume, concentration and injection rate of contrast medium (Bae KT, 2010; Herman S, 2004). Various contrast media with different iodine concentration including Angio-Conray, Ioverin, Iohexol and Iopromide were used in previous studies (Lawrentschuk N *et al*., 2005; Liu Y *et al*., 2012; Tanaka T *et al*., 2019; Yamazoe K *et al*., 1994) that caused different post-contrast attenuation value. Considering the variability of body size and injection-related factors, including various contrast media and their effect on attenuation values, what is needed is not only quantitative measurement of attenuation values but also qualitative evaluation of contrast enhancement. Therefore, this study evaluated the contrast enhancement tendency of renal tumors using triphasic contrast-enhanced CT to compare various renal tumors.

In this study, triphasic post-contrast images at 20, 40 and 60 s after contrast medium injection were evaluated. In dogs, few CT studies were reported for optimizing renal phases including corticomedullary, nephrographic and excretory phases (Cho H *et al*., 2018; Lee S *et al*., 2011). The corticomedullary phase is

characterized by renal cortex enhancement rather than the medulla, whereas the nephrographic phase shows homogeneous opacification of the renal cortex and medulla. The excretory phase is defined as excretion of urine (Cho H *et al*., 2018). In previous contrast-enhanced CT study in normal dogs, the optimal scan times for corticomedullary, nephrographic and excretory phases were 10, 44, and 65 s after contrast medium injection (Cho H *et al*., 2018), whereas the results of other study were 5, 10, and 30 s after aorta triggering at 100 HU (Lee S *et al*., 2011). Optimal scans for corticomedullary, nephrographic and excretory phases were not performed in this study due to its retrospective nature, however, triphasic post-contrast images were consistent with the definition of corticomedullary, nephrographic and excretory phases and scan times were similar to previous study (Cho H *et al*., 2018).

RCC was the most common renal tumor in this study as in previous canine studies (Morris J and Dobson J, 2001). Canine RCC are classified into several subtypes, including clear cell, chromophobe, papillary and multilocular cystic RCC, based on histologic features and histochemical and immunohistochemical staining (Edmondson EF *et al*., 2015). In dogs, papillary RCC has high incidence comprising a majority of RCC, following clear cell or chromophobe RCC (Edmondson EF *et al*., 2015). Contrast-enhanced CT studies in human, papillary RCC usually appears homogeneous and hypovascularized mass with progressive contrast enhancement (Kim SH *et al*., 2016; Muglia VF and Prando A, 2015). Renal clear cell carcinoma shows heterogeneous and hypervascularized lesions with strong contrast enhancement in the corticomedullary phase and typically decreasing attenuation in the nephrographic phase (Kim *et al*., 2016; Muglia VF and Prando A, 2015). Chromophobe RCC shows contrast enhancement values between papillary and clear cell RCC in corticomedullary phase with decreased values in the excretory phase (Kim SH *et al*., 2016). RCC was not subdivided in this study, however, all dogs with RCC showed progressive contrast enhancement from pre-contrast to nephrographic phase, similar to papillary or chromophobe RCC in humans, whereas the major contrast enhancement patterns were heterogeneous. These results were similar to previous contrast-enhanced CT studies in dogs with RCC (Tanaka T *et al*., 2019). Further triphasic CT studies with large cases of canine RCC with subtype are needed to determine contrast enhancement characteristics for each subtype.

In dogs and humans, renal lymphoma typically shows homogeneous and hypoattenuation or slight hyperattenuation on pre-contrast CT images with homogeneously poor contrast enhancement (Sheth S *et al*., 2006; Tanaka T *et al*., 2019). Lymphomatous deposits can lead to hypovascularization producing lower attenuation with lesser enhancement (Sheth S *et al*., 2006). In the present study, both cats with renal lymphoma showed hypoattenuating renal mass on pre-contrast CT and relatively gradual, progressive heterogeneous contrast enhancement from corticomedullary to the excretory phase. This discrepancy of contrast enhancement pattern between ours and previous studies could be due to the degree of renal infiltration by malignant lymphocytes. In humans, the diffuse infiltration of malignant lymphocytes on the renal interstitium leads to nephromegaly without distortion of the normal renal shape (Sheth S *et al*., 2006; Urban BA and Fishman EK, 2020). Infiltrative renal lymphoma presents global renal enlargement with heterogeneous contrast enhancement on contrast-enhanced CT with renal sinus fat infiltration, which is similar to our patients (Sheth S *et al*., 2006; Urban BA and Fishman EK, 2020). Further research is required with large cases to characterize CT features and its enhancement pattern in feline renal lymphoma.

Nephroblastoma is an uncommon tumor and is mostly reported in relatively young dogs (Bryan JN *et al*., 2006; Montinaro V *et al*., 2013; Yamazoe K *et al*., 1994). In dogs, only 2 CT cases were reported for nephroblastoma (Montinaro V *et al*., 2013; Yamazoe K *et al*., 1994). In these previous reports, pre-contrast CT findings are described differently as hypoattenuating or slightly hyperattenuating mass compared to normal renal parenchyma with or without calcification. These masses revealed mild contrast enhancement on post-contrast CT (Montinaro V *et al*., 2013; Yamazoe K *et al*., 1994). However, contrast-enhanced CT scan times are unclear, described as few hours after pyelography or not. In our case of nephroblastoma, hypoattenuating and heterogeneous renal mass with plateau contrast enhancement pattern was identified. In addition, invasion to caudal vena cava and lymphadenopathy were observed. In humans, CT characteristics of nephroblastoma are expansible with or without cystic components, poor margination, calcification, hemorrhage, vascular invasion and lymphadenopathy, and is hypoattenuating or isoattenuating compared to a renal cortex with poor contrast enhancement (Wu J *et al*., 2016). In addition, attenuation values of each corticomedullary, nephrographic and delayed phases are relatively in a plateau pattern (Wu J *et al*., 2016). These CT characteristics were similar to our case. Only one dog was included in this study, however, this is the first triphasic CT report of canine nephroblastoma and its findings will be helpful in future diagnostic imaging studies of canine renal tumor.

Vascular invasion was detected in 14.3% of dogs with RCC and one nephroblastoma case and all dogs had caudal vena cava invasion only. In prior studies in dogs with primary renal cell tumor including RCC, lymphoma, and hemangiosarcoma, only one dog with RCC (11% of RCC cases) had vena cava infiltration, showing a similar rate to our study (Tanaka T *et al*., 2019). In humans, the tumor extension into the renal vein or vena cava does not significantly affect prognosis after nephrectomy with and without cavotomy (Ficarra V *et al*., 2001), whereas the prognostic value of the presence of vascular invasion in dogs with renal tumor is still unknown.

Pulmonary metastasis is reported in 16%–26.7% in dogs with primary renal tumor at diagnosis (Bryan JN *et al*., 2006; Tanaka T *et al*., 2019). In this study, pulmonary metastasis was identified in 50% dogs, of which 3 were RCC and one was nephroblastoma. In previous studies, pulmonary metastasis was detected in 17.6%–48% of dogs with RCC (Bryan JN *et al*., 2006; Edmondson EF *et al*., 2015; Tanaka T *et al*., 2019), which

was lower than our cases. In nephroblastoma, pulmonary metastasis is detected in 20% of cases, but the number of dogs included is small (Bryan JN *et al*., 2006). Considering the shorter survival time than previous studies, which shows median survival time of 16 months in RCC, 6 months in nephroblastoma (Bryan JN *et al*., 2006), and 3–6 months in lymphoma with chemotherapy (Vail DM *et al*., 1998), the higher pulmonary metastasis in this study is thought to be due to the later diagnosis after renal tumor progression.

There were several limitations of the present study. First, the number of patients included in this study was too small for statistical comparison. Second, optimal CT scans for corticomedullary, nephrographic and excretory phases were not performed due to the retrospective nature. Third, histopathologic classifications of RCC subtypes and cytohistologic examination of pulmonary nodules were not performed. However, this study is valuable since it describes the triphasic CT characteristics of renal tumor in dogs and cats. In addition, this is the first triphasic CT report of canine nephroblastoma.

In conclusion, triphasic CT examination could be helpful in renal tumor characterization and vascular invasion and metastasis evaluation. Further large-scale, standardized triphasic CT studies with various renal tumors are needed to figure out the association between CT and histopathological findings.

References

Bae KT 2010. Intravenous contrast medium administration and scan timing at CT: considerations and approaches. Radiol. 256: 32-61.

Bertolotto M, Bucci S, Valentino M, Currò F, Sachs C, Cova MA 2018. Contrast-enhanced ultrasound for characterizing renal masses. Eur J Radiol. 105: 41-48.

Bryan JN, Henry CJ, Turnquist SE, Tyler JW, Liptak JM, Rizzo SA, Sfiligoi G, Steinberg SJ, Smith AN, Jackson T 2006. Primary renal neoplasia of dogs. J Vet Intern Med. 20: 1155-1160.

Cho H, Lee DH, Cha AY, Kim DE, Chang DW, Choi J 2018. Optimization of scan delay for multi-phase computed tomography by using bolus tracking in normal canine kidney. J Vet Sci. 19: 290-295.

Crow SE 1985. Urinary tract neoplasms in dogs and cats. Comp Cont Educ Pract. 7 : 607-618.

Edmondson EF, Hess, AM, Powers BE 2015. Prognostic significance of histologic features in canine renal cell carcinomas: 70 nephrectomies. Vet Pathol. 52: 260-268.

Ficarra V, Righetti R, D'Amico A, Rubilotta E, Novella G, Malossini G, Mobilio G 2001. Renal vein and vena cava involvement does not affect prognosis in patients with renal cell carcinoma. Oncology. 61: 10-15.

Haers H, Vignoli M, Paes G, Rossi F, Taeymans O, Daminet S, Saunders JH 2010. Contrast harmonic ultrasonographic appearance of focal space-occupying renal lesions. Vet Radiol Ultrasound. 51: 516-522.

Herman S 2004. Computed tomography contrast enhancement principles and the use of high-concentration contrast media. J Comput Assist Tomogr. 28: S7-11.

Kim SH, Kim CS, Kim MJ, Cho JY, Cho SH 2016. Differentiation of clear cell renal cell carcinoma from other subtypes and fat-poor angiomyolipoma by use of quantitative enhancement measurement during three-phase MDCT. AJR Am J Roentgenol. 206: W21-28.

Lawrentschuk N, Gani J, Riordan R, Esler S, Bolton DM 2005. Multidetector computed tomography vs magnetic resonance imaging for defining the upper limit of tumor thrombus in renal cell carcinoma: a study and review. BJU Int. 96: 291-295.

Lee S, Jung J, Chang J, Yoon J, Choi M 2011. Evaluation of triphasic helical computed tomography of the kidneys in clinically normal dogs. Am J Vet Res. 72: 345-349.

Liu Y, Song T, Huang Z, Zhang S, Li Y 2012. The accuracy of multidetector computed tomography for preoperative staging of renal cell carcinoma. Int Braz J Urol. 38: 627-636.

Montinaro V, Boston SE, Stevens B 2013. Renal nephroblastoma in a 3-month-old golden retriever. Can Vet J. 54: 683-686.

Mooney SC, Hayes AA, Matus RE, MacEwen EG 1987. Renal lymphoma in cats: 28 cases (1977–1984). J Am Vet Med Assoc. 191: 1473-1477.

Morris J, Dobson J 2001. Small animal oncology. Oxford: Blackwell Science. 154-165.

Muglia VF, Prando A 2015. Renal cell carcinoma: histological classification and correlation with imaging findings. Radiol Bras. 48: 166-174.

Sheth S, Ali S, Fishman E 2006. Imaging of renal lymphoma: patterns of disease with pathologic correlation. Radiographics. 26: 1151-1168.

Tanaka T, Akiyoshi H, Nishida H, Mie K, Lin LS, Iimori Y, Okamoto M 2019. Contrast-enhanced computed tomography findings of canine primary renal tumors including renal cell carcinoma, lymphoma, and hemangiosarcoma. PLoS One. 14: e0225211.

Urban BA, Fishman EK 2020. Renal lymphoma: CT patterns with emphasis on helical CT. Radiographics. 20: 197-212.

Vail DM, Moore AS, Ogilvie GK, Volk LM 1998. Feline lymphoma (145 cases): proliferation indices, cluster of differentiation 3 immunoreactivity, and their association with prognosis in 90 cats. J Vet Intern Med. 12: 349-354.

Wu J, Zhu Q, Zhu W, Chen W 2016. CT and MRI imaging features and long-term follow-up of adult Wilms' tumor. Acta Radiol. 57: 894-900.

Yamazoe K, Ohashi F, Kadosawa T, Nishimura R, Sasaki N, Takeuchi A 1994. Computed tomography on renal masses in dogs and cats. J Vet Med Sci. 56: 813-816.

Yuh BI, Cohan RH 1999. Different phases of renal enhancement: role in detecting and characterizing renal masses during helical CT. AJR Am J Roentgenol. 173: 747-755.